

# Coulomb and nuclear breakup of three-body halo nuclei

E. GARRIDO<sup>1</sup>, D.V. FEDOROV<sup>2</sup> and A.S. JENSEN<sup>2</sup>

<sup>1</sup> *Instituto de Estructura de la Materia, CSIC - Serrano 123, E-28006 Madrid, Spain*

<sup>2</sup> *Institute of Physics and Astronomy, Aarhus University - DK-8000 Aarhus C, Denmark*

PACS. 25.10.+s – Nuclear reactions involving few-nucleon systems.

PACS. 25.60.Gc – Breakup and momentum distributions.

**Abstract.** – We investigate dissociation reactions of loosely bound and spatially extended three-body systems. We formulate a practical method for simultaneous treatment of long-range Coulomb and short-range nuclear interactions. We use  ${}^6\text{He}$  ( $n+n+\alpha$ ) and  ${}^{11}\text{Li}$  ( $n+n+{}^9\text{Li}$ ) as examples and study the two-neutron separation cross sections as functions of target and beam energy. Individual Coulomb and nuclear as well as interference contributions are also extracted.

*Introduction.* – Nuclear halos were discovered by their surprisingly large reaction cross sections with ordinary target nuclei [1–5]. Most of the information about these unusual structures are obtained by detailed fragmentation reaction studies [6–10]. The understanding of these halo systems is based on an effective clustering into few-body structures reacting with the target. The main structure is essentially agreed upon as two or three-body systems with  ${}^{11}\text{Be}$  ( $n+{}^{10}\text{Be}$ ) as the prototype of a two-body halo and  ${}^6\text{He}$  ( $n+n+\alpha$ ) and  ${}^{11}\text{Li}$  ( $n+n+{}^9\text{Li}$ ) as three-body halos [11].

The reaction description is much less advanced and are mostly available as fragmentary computations where one quantity is investigated in one particular model with one set of parameters [5, 12–16]. Systematic and consistent calculations of many observables within one model are highly desired but scarce [17]. The difficulties in an accurate treatment are substantial, since even when the constituent clusters and the target are oversimplifyingly considered to be point-like, the reactions still involve three and four-body systems for two and three-body halos, respectively. Approximations are therefore inevitable.

One of the major problems in obtaining fragmentation cross sections is to incorporate Coulomb and nuclear interactions in the same numerical procedure [5, 18]. This has been attempted for two-body projectiles [19, 20] while three-body projectiles at best are treated as effective two-body systems [5, 18] or by computing the Coulomb and nuclear contributions in independent models [5, 15, 18, 21, 22]. This situation is rather unsatisfactory, since breakup reactions of nuclear halos are dominated by nuclear and Coulomb interactions for light and heavy nuclear targets, respectively [5, 18, 22].

Significant improvements can be expected to be difficult, especially for three-body projectiles, since a mixture of long-range and short-range interactions is involved. The efforts may also be very rewarding first by allowing the necessary treatment of specific reactions and

second due to the general nature of the problem and the derived interest from other subfields of physics. We formulate in this report a practical method to include Coulomb and nuclear interactions simultaneously in investigations of breakup reactions of three-body halo nuclei.

*Model assumptions.* – We consider a three-body halo system colliding with a target. We assume first that the intrinsic motion of the halo is slow compared to the relative projectile-target motion. The three-body system does not have time to adjust to the external field during the collision and the sudden approximation therefore applies. For point-like particles each halo particle, called the participant, can then interact with the target without disturbing the motion of the other two, called spectators. We can then treat the reaction as independent collisions and the total cross section is the sum of contributions from the three participants. Apart from energy and momentum conservation and overlaps between initial and final states of the spectators we are then left with three independent two-body problems. The corresponding interactions should then describe these two-body collisions to the required level of accuracy. We use the phenomenological optical model designed to describe elastic scattering and absorption from the elastic channel.

The finite extension of both target and halo particles demands additional considerations, since simultaneous collisions of more than one halo particle then could be quite frequent in contradiction to our basic assumption. Therefore in addition to the detailed treatment of the essential contribution of the participant we use the simpler “black sphere” model to describe the smaller contributions from the spectators. If the spectators are able to pass without touching the target they are true spectators and otherwise they are counted as absorbed by the target and consequently removed from the final state. This is the optical model limit of very strong absorption for short-range potentials. This division into detailed treatment of participant and use of the black sphere for the spectators is only meaningful when the halo is larger than the combined sizes of the target and the participant. This is similar to the assumption used in the formulation for a weakly bound projectile [23]. A better treatment of the collision between three-body halos and a target almost inevitably has to deal with more than three-body configurations in the final state or include properties of the intrinsic structure of the halo particles and the target.

*Method.* – The finite extension of the projectile particles and the target destroy the clear division into participant and spectators, since the spectators may hit the target in the same collision where the participant is scattered or absorbed. We start by treating the interaction between the target and the projectile constituents in the black sphere model where the particle is absorbed inside a cylinder with the axis along the beam direction and left untouched outside this cylinder of a radius approximately equal to the target plus spectator radius. If  $P_c$ ,  $P_{n1}$  and  $P_{n2}$  are the probabilities for the core, first and second neutron being inside this cylinder the reaction probability is the sum of the probabilities of finding all three constituents inside the cylinders ( $P_{n1}P_{n2}P_c$ ), plus the probability of finding two constituents inside (three terms like  $P_iP_j(1 - P_k)$ ), plus the probability of finding only one constituent inside the cylinder (three terms like  $P_i(1 - P_j)(1 - P_k)$ ). We then consider all possible combinations in the projectile-target interaction. The sum of all these terms give the reaction probability, that can be rewritten as  $P_c + P_{n1}(1 - P_c) + P_{n2}(1 - P_c)(1 - P_{n1})$ . Each term in this probability vanishes unless one particular projectile constituent is inside the cylinder. This is the constituent chosen as participant, while the other two are considered spectators. The optical model is then used for the participant-target interaction.

*Participant treatment.* – We consider collisions for an initial velocity  $v$ , the corresponding momentum  $p$ , and total kinetic energy of  $EA$ , where  $A$  is the mass number of the projectile.

The target (labeled 0) has charge  $Z_0$  and mass  $m_0$ , the participant (labeled  $i$ ) has charge  $Z_i$  and mass  $m_i$ . We label the spectators by  $j$  and  $k$ , final state quantities by primes, relative two-body coordinates and momenta between particles  $i$  and  $k$  by  $\mathbf{r}_{ik}$  and  $\mathbf{p}_{ik}$  and between  $i$  and the center of mass of  $j$  and  $k$  by  $\mathbf{r}_{i,jk}$  and  $\mathbf{p}_{i,jk}$ . The initial wave function is a product of the three-body wave function and a plane wave describing the relative halo-target motion. The final state wave function is a product of three terms, i.e. two distorted waves for the participant-target and the spectator-spectator motion and a plane wave for the relative motion of these two non-interacting two-body systems. The distorted waves are obtained by solving the Schrödinger equation with the appropriate two-body potentials.

The cross section of the participant  $i$  has two contributions corresponding to elastic scattering (diffraction) and absorption (stripping). The differential diffraction cross section reduces to a factorized form when the participant has spin 0 or 1/2 and the target has spin 0 [17]

$$\frac{d^9 \sigma_{el}^{(i)}(\mathbf{p}'_{0i,jk}, \mathbf{p}'_{jk}, \mathbf{p}'_{0i})}{d\mathbf{p}'_{0i,jk} d\mathbf{p}'_{jk} d\mathbf{p}'_{0i}} = \frac{d^3 \sigma_{el}^{(0i)}(\mathbf{p}_{0i} \rightarrow \mathbf{p}'_{0i})}{d\mathbf{p}'_{0i}} \times (1 - |\langle \Psi | \exp(i\delta\mathbf{q} \cdot \mathbf{r}_{i,jk}) | \Psi \rangle|^2) |M_s(\mathbf{p}_{i,jk}, \mathbf{p}'_{jk})|^2, \quad (1)$$

where  $\mathbf{p}'_{0i,jk} = \mathbf{p}_{i,jk} + \mathbf{p}_0(m_j + m_k)/(m_0 + m_i + m_j + m_k)$  in the rest frame of the projectile,  $\Psi$  is the initial three-body halo state,  $\delta\mathbf{q} = (\mathbf{p}'_{i,jk} - \mathbf{p}_{i,jk})(m_j + m_k)/(m_i + m_j + m_k)$  is the momentum transfer into the relative participant-spectators motion and  $M_s(\mathbf{p}_{i,jk}, \mathbf{p}'_{jk})$  is the normalized overlap matrix element between initial and final state spectator wave functions.

The first factor,  $d^3 \sigma_{el}^{(0i)}(\mathbf{p}_{0i} \rightarrow \mathbf{p}'_{0i})/d\mathbf{p}'_{0i}$ , is the differential cross section for the participant-target elastic scattering process. It is obtained by numerical computation of the phase shifts including simultaneously the nuclear and Coulomb potential. At small momentum transfers (large impact parameters) or large angular momenta the Rutherford cross section is approached as the effect of the short-range nuclear interaction then disappears.

The second factor in Eq.(1) is constructed as one minus the probability for staying in the ground state after transfer of the momentum  $\delta\mathbf{q}$  in the reaction, i.e. we remove the probability for elastic scattering of the halo as a whole. This could alternatively be done by orthogonalizing the final state in the overlap matrix element to the initial three-body ground state.

Collisions at sufficiently large impact parameters only produce virtual excitations corresponding to adiabatic motion [5, 18]. The limiting impact parameter  $b_a$  is determined by equating the reaction time  $2b_a/v$  with the time period  $2\pi\hbar/B_{ps}$  in the relative motion of the participant-spectators system with the corresponding binding energy  $B_{ps}$ . The Coulomb interaction then transfers the momentum  $q_a = Z_0 Z_i e^2 p / (b_a A E) = Z_0 Z_i e^2 / (\pi c) B_{ps} / (\hbar c) (\gamma + 1) \gamma^{-2} \beta^{-2}$ , where  $\beta = v/c$  and  $\gamma = 1/\sqrt{1 - \beta^2}$ .

The energy transferred from target to participant,  $\delta E \equiv \sqrt{\mathbf{p}_0^2 + m_0^2} - \sqrt{\mathbf{p}'_0{}^2 + m_0^2}$ , must be larger than the three-body separation energy  $B$ . When  $\mathbf{p}_0$  and  $\mathbf{q} \equiv \mathbf{p}_0 - \mathbf{p}'_0$  are parallel  $\delta E$  is maximized. For this geometry we find for small  $B$  compared to the target rest mass that  $\delta E = B$  implies that  $qc \equiv q_L c \approx B \sqrt{1 + m_0^2 c^2 / p_0^2}$  which reduces to  $B/v$  in the non-relativistic limit. Thus  $q$  must be larger than  $q_L$  to produce dissociation, but on the other hand dissociation is not the necessary outcome for all  $q > q_L$ . We exclude contributions from momentum transfer smaller than the largest of  $q_L$  and  $q_a$ .

The differential absorption (stripping) cross section, where the participant in the sense of

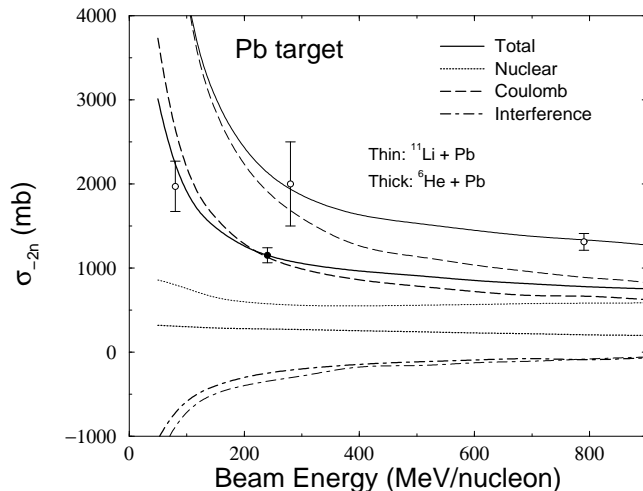


Fig. 1 – Two-neutron removal cross sections as functions of beam energy for fragmentation of  ${}^6\text{He}$  (thick) and  ${}^{11}\text{Li}$  (thin) on a Pb-target. We show the total cross section (solid) as well as contributions from Coulomb (dashed), nuclear (dotted) and interference terms (dot-dashed). The curves for  ${}^6\text{He}$  are lower than those of  ${}^{11}\text{Li}$ . The experimental data are from [6–8, 10],  ${}^{11}\text{Li}$  (open circles) and  ${}^6\text{He}$  (filled circles).

the optical model is absorbed by the target, is obtained analogously [17]

$$\frac{d^6\sigma_{abs}^{(i)}(\mathbf{p}'_{0i,jk}, \mathbf{p}'_{jk})}{d\mathbf{p}'_{0i,jk} d\mathbf{p}'_{jk}} = \sigma_{abs}^{(0i)}(p_{0i}) |M_s(\mathbf{p}_{i,jk}, \mathbf{p}'_{jk})|^2, \quad (2)$$

where  $\sigma_{abs}^{(0i)}$  is the participant-target absorption cross section. The nine-dimensional differential cross section is now reduced to six, since the absorbed or stripped particle inherently is of no interest in the optical model description. The factorizations in both Eqs.(1) and (2) are incomplete, since  $\mathbf{p}_{0i}$  via momentum conservation is related to  $\mathbf{p}'_{0i,jk}$  and  $\mathbf{p}_{i,jk}$ .

The total differential cross section for any reaction is now obtained by adding the two contributions from scattering and absorption to analogous contributions when particles  $j$  and  $k$  are the participants. All these contributions are given on an absolute scale and their relative weights are therefore determined in this model. We integrate over all unobserved momenta in Eqs.(1) and (2).

*Spectator treatment.* – The spectator-target interaction is treated in the black sphere model. This model can be implemented by considering the distance  $r_{ps}$  between the participant and the spectator [17]. When  $r_{ps}$  is small participant and spectator both would for short-range interactions interact with the target, and therefore according to the black sphere model the spectator would be absorbed. The distance  $r_{ps}$  is then determining if the spectator is either absorbed (distances smaller than  $r_{ps}$ ) or undisturbed (distances larger than  $r_{ps}$ ). The absorption distances  $r_{ps}$  [17] are related to the sizes of target and spectators and determined by  $\frac{3}{5}r_{ps}^2 = \langle r^2 \rangle_t + \langle r^2 \rangle_s + 2 \text{ fm}^2$ , where  $\langle \rangle$  is the measured mean square radius of target or spectator and  $2 \text{ fm}^2$  is the square of the range of the nucleon interaction. These radii  $r_{ps}$  can also be obtained from the parametrization in Eq.(28) of [17] with  $r_0 = 1.26 \text{ fm}$ ,  $1.30 \text{ fm}$  and  $1.45 \text{ fm}$  for the targets Pb, Cu and C, respectively. In the same way when the charged

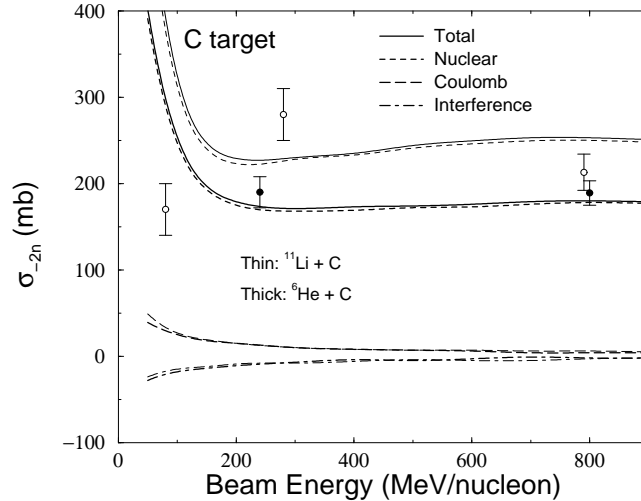


Fig. 2 – The same as Fig. 1 for a Carbon target. The experimental data are from [3, 7, 8, 10].

participant is absorbed in the optical model sense, it must have been close to the target and close-lying spectators within the absorption distance must also be counted as absorbed. On the other hand when the charged participant is scattered small momentum transfer corresponds to a large impact parameter. These events only occur when the distance between participant and target is large and it is then very unlikely that spatially close-lying spectators are absorbed. All spectators are therefore counted as scattered. For large momentum transfer in the scattering process corresponding to impact parameters smaller than the sum of target and participant radii the spectator is analogously counted as absorbed. For two-neutron dissociation cross sections this division is irrelevant, since these contributions all are included in the cross section.

*Results.* – We apply the procedure on the prominent nuclear three-body halos  ${}^6\text{He}$  and  ${}^{11}\text{Li}$ . The neutron-neutron and the neutron-core two-body interaction parameters are given in [16, 17]. The optical model parameters are from [24] for the neutrons, from [25] for  $\alpha$ -particles and for  ${}^9\text{Li}$ -particles from [25] with range and diffuseness parameters from [26]. We furthermore drastically reduce the energy dependence of the real potential in [25] to allow for the required huge beam energy variation, i.e.  $a_2 = -0.014$ . The measured core-target interaction cross sections are reproduced within error bars [7]. The binding energy  $B_{ps}$  between the  ${}^9\text{Li}$  and  ${}^4\text{He}$  cores and the two neutrons must be introduced for the low momentum cutoff. We use the scaling relation in [27] to obtain  $B_{ps}/B \approx 3$  for  ${}^6\text{He}$  and 1.4 for  ${}^{11}\text{Li}$ . The two-neutron dissociation cross sections are shown in fig. 1 as functions of beam energy for a Pb-target. The theoretical uncertainties are mostly due to the inaccurate optical model. Also the precise choice of cutoff parameter gives an uncertainty on the Coulomb part, especially important at higher energies. For Pb the adiabatic cutoff is the largest and therefore decisive, i.e.  $q_a > q_L$ . The  ${}^{11}\text{Li}$  results are larger than those of  ${}^6\text{He}$  because the Coulomb contribution roughly scales with the square of the projectile charge and the nuclear part increases with the projectile size. The small nuclear part has contributions from both neutron and core as participants. They both decrease up to about 200 MeV/nucleon then remaining roughly constant at higher energies. Discussions of the individual behavior of the

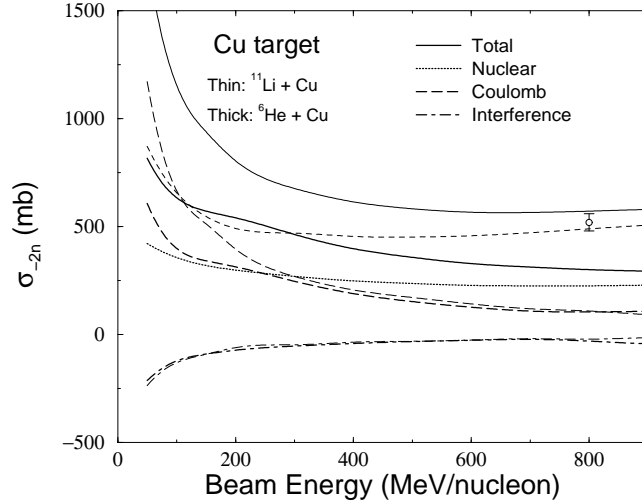


Fig. 3 – The same as fig. 1 for a Copper target. The experimental point for  $^{11}\text{Li}$  is from [6].

many contributions are not possible here. The dominating Coulomb contributions decrease with energy first strongly and then much slower above 200 MeV/nucleon. The interference terms are negative and rather small, but significant at low energies, where the total cross section is below the Coulomb contribution. The measured values are reproduced at high energies but exceeded by a factor of two at low energy as already noticed in [17]. Our results are consistent with estimates reported in [12].

The trends for the individual terms are roughly the same for C as for Pb, see fig. 2. The nuclear parts increase slowly with energy above 200 MeV/nucleon. The adiabatic cutoff is now the smallest and therefore  $q_L$  is decisive, i.e.  $q_a < q_L$ . We observe a small increase of the total cross section with increasing energy. The nuclear contributions are completely dominating for a light target and the numerical values are therefore also very similar for both projectiles. Again we do not reproduce the (inconsistent) experimental data at lower energies.

Coulomb and nuclear contributions are comparable for a medium heavy target, see fig. 3. The two cutoff parameters are now comparable and  $q_a$  is decisive at small energies whereas  $q_L$  becomes larger at higher energies. The trends for the individual terms still remain the same as for C and Pb. Now the decreasing Coulomb contribution crosses the almost energy independent nuclear contribution at about 300 MeV/nucleon for  $^6\text{He}$  and at 200 MeV/nucleon for  $^{11}\text{Li}$ . The interference terms are still rather small except at low energies.

*Conclusion..* – We have formulated a method to compute dissociation cross sections of loosely bound three-body systems interacting with a mixture of short and long-range potentials. The uncertainties in the numerical results are dominated by the uncertainties in the two-body optical potentials for light targets and in the cutoff parameter for heavy targets. The already rather heavy computations seem to suffice as seen by comparing with the measurements. The present consistent and systematic calculations may prove useful as a guide for future experimental investigations. The dissociation cross sections are for example predicted to increase as the beam energy decreases below 200 MeV/nucleon and slowly decrease or increase with increasing energy for higher energies, respectively for heavy and light targets.

\* \* \*

We thank K. Riisager for continuous discussions and suggestions.

## REFERENCES

- [1] RIISAGER K., *Rev. Mod. Phys.*, **66** (1994) 1105.
- [2] HANSEN P.G., JENSEN A.S. and JONSON B., *Ann. Rev. Nucl. Part. Sci.*, **45** (1995) 591.
- [3] TANIHATA I., *J. Phys. G*, **22** (1996) 157.
- [4] JONSON B. and RIISAGER K., *Phil. Trans. R. Soc. Lond. A*, **356** (1998) 2063.
- [5] BERTULANI C.A., CANTO L.F. and HUSSEIN M.S., *Phys. Rep.*, **226** (1993) 281.
- [6] KOBAYASHI T. ET AL., *Phys. Lett. B*, **232** (1989) 51.
- [7] BLANK B. ET AL., *Nucl. Phys. A*, **555** (1993) 408.
- [8] ZINSER M. ET AL., *Nucl. Phys. A*, **619** (1997) 151.
- [9] ALEKSANDROV D. ET AL., *Nucl. Phys. A*, **633** (1998) 234.
- [10] AUMANN T. ET AL., *Phys. Rev. C*, **59** (1999) 1252.
- [11] ZHUKOV M.V. ET AL., *Phys. Rep.*, **231** (1993) 151.
- [12] OGAWA Y., YABANA K. and SUZUKI Y., *Nucl. Phys. A*, **543** (1992) 722.
- [13] SUZUKI Y., KIDO T., OGAWA Y., YABANA K. and BAYE D., *Nucl. Phys. A*, **567** (1994) 957.
- [14] BERTSCH G.F., HENCKEN K. and ESBENSEN H., *Phys. Rev. C*, **57** (1998) 1366.
- [15] BANERJEE P., TOSTEVIN J.A. and THOMPSON I.J., *Phys. Rev. C*, **58** (1998) 1337.
- [16] COBIS A., FEDOROV D.V. and JENSEN A.S., *Phys. Rev. C*, **58** (1998) 1403.
- [17] GARRIDO E., FEDOROV D.V. and JENSEN A.S., *Phys. Rev. C*, **59** (1999) 1272.
- [18] BERTULANI C.A. and BAUR G., *Phys. Rep.*, **163** (1988) 299.
- [19] DASSO C., LENZI S.M. and VITTURI A., *Nucl. Phys. A*, **639** (1998) 635.
- [20] SHYAM R. and THOMPSON I.J., *Phys. Rev. C*, **59** (1999) 2645.
- [21] BERTULANI C.A., BAUR G. and HUSSEIN M.S., *Nucl. Phys. A*, **526** (1991) 751.
- [22] BANERJEE P. and SHYAM R., *Nucl. Phys. A*, **561** (1993) 112.
- [23] BANG J. and PEARSON C.A., *Nucl. Phys. A*, **100** (1967) 1.
- [24] COOPER E.D., HAMA S., CLARK B.C. and MERCER R.L., *Phys. Rev. C*, **47** (1993) 297.
- [25] NOLTE M., MACHNER H. and BOJOWALD J., *Phys. Rev. C*, **36** (1987) 1312.
- [26] ZAHAR M. ET AL., *Phys. Rev. C*, **54** (1996) 1262.
- [27] JOHANNSEN L., JENSEN A.S. and HANSEN P.G., *Phys. Lett. B*, **244** (1990) 357.